

Phase Transitions and Duality in Adiabatic Memristive Networks

Forrest C. Sheldon* and Massimiliano Di Ventra†

Department of Physics, University of California San Diego, La Jolla, California 92093, USA

(Dated: August 12, 2016)

The development of neuromorphic systems based on memristive elements - resistors with memory - requires a fundamental understanding of their collective dynamics when organized in networks. Here, we study an experimentally inspired model of two-dimensional disordered memristive networks subject to a slowly ramped voltage and show that they undergo a first-order phase transition in the conductivity for sufficiently high values of memory, as quantified by the memristive ON/OFF ratio. We investigate the consequences of this transition for the memristive current-voltage characteristics both through simulation and theory, and uncover a duality between forward and reverse switching processes that has also been observed in several experimental systems of this sort. Our work sheds considerable light on the statistical properties of memristive networks that are presently studied both for unconventional computing and as models of neural networks.

INTRODUCTION

Although systems that display resistive switching - also referred to as “memristive elements” (resistors with memory) - have been actively studied since the 1960s, they have recently received renewed interest in view of their possible use in computation, both as logic and memory components [1]. Of particular note is the tendency of some to display a history-dependent decay constant, allowing a transition between a volatile and non-volatile regime of memory [2, 3]. The resulting dynamics bear a close resemblance to the short-term and long-term potentiation observed in biological synapses which are thought to be of central importance to learning and plasticity in the brain [4]. This resemblance has inspired the realization of experimental systems that seek to combine the memory features of biological synapses with the structural complexity of neural tissue [5, 6]. In fact, research is being performed to assess the advantage of using memristive elements in non-von Neumann architectures and is already showing that their networks dynamically organize into the solutions of complex computational problems, thereby performing the computation directly in the memory and avoiding the separation between logic and memory units [7–10].

All of these studies however, still lack a fundamental understanding of the role of time non-locality in the dynamics of memristive networks and their statistical properties. For instance, high density ($\sim 10^9$ elements/cm²) disordered networks of memristive Ag/Ag₂S/Ag atomic switches have been fabricated showing collective switching behavior between a low-resistance (G_{on}) and high-resistance (G_{off}) state, and possible critical states potentially useful in neuromorphic computation [4, 11, 12]. Some theoretical work has attempted to reproduce several features observed in the experiments by performing simulations in relatively small networks but an understanding of the dynamics of such systems is far from clear [13, 14]. Theoretical investigations of one-dimensional memristive networks have shown complex temporal dy-

namics and scale-invariant properties, but have not clarified whether further collective behavior might arise in higher dimensions [15].

To fill this gap, we study the statistical properties of two-dimensional disordered memristive networks subject to a slowly ramped voltage. In this ‘adiabatic’ regime, where the applied voltage/current varies much more slowly than the memristance change of individual elements, there is a strong analogy between the behavior of the network and an equilibrium thermal system. Our aim is to understand the dynamics of both the disordered devices being assembled in experiment, and the ordered (but strongly heterogeneous) networks being proposed as novel computational architectures. To this end, we formulate a general model for networks in this limit which is similar to those employed to describe metal-insulator transitions and electrical failure. We thus posit that the transitions identified in these fields should also occur in memristive networks and summarize work done to describe the dynamics in these fields. Through simulations we obtain current-voltage (I-V) curves for various values of the G_{on}/G_{off} ratio and discuss the features implied by the adiabatic limit. The I-V curves found show a duality between forward and reverse switching processes that has been observed in several experimental systems [16, 17] and clarifies the role of boundary conditions in the network. These features are captured by a mean-field theory and cluster approximation which clarify the internal dynamics and account for the features of the I-V curves. These results shed considerable light on the statistical and collective properties of networks with memristive elements that are being currently explored for neuromorphic applications.

MODEL

As inspiration and as a test bed for disordered memristive networks we consider the Ag/Ag₂S/Ag gapless atomic switches experimentally fabricated in [5, 6, 18].

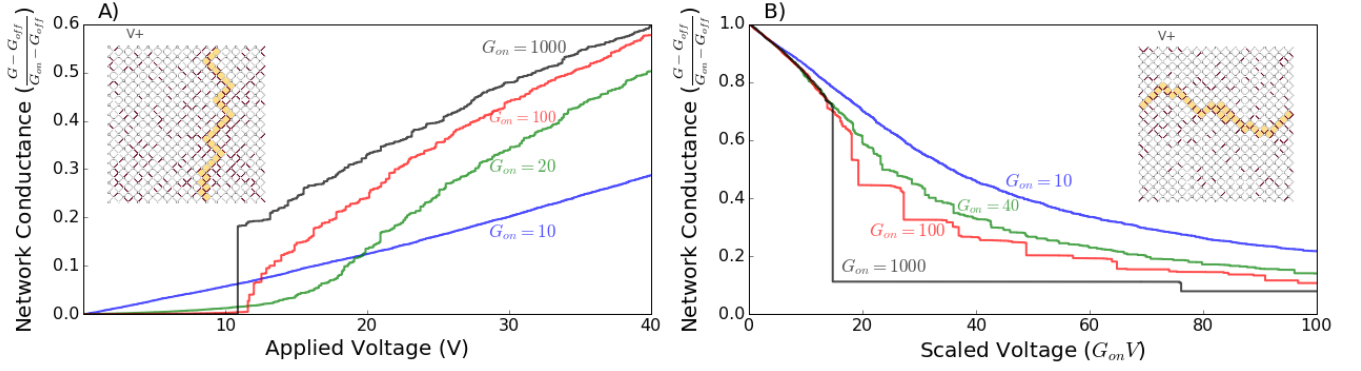


FIG. 1. The network conductance for several values of G_{on} are plotted against the applied voltage for both (A) $G_{off} \rightarrow G_{on}$ and (B) $G_{on} \rightarrow G_{off}$. The network conductance G has been scaled to vary from 0 to 1 and the range of the applied voltage shortened to focus on the point of transition. The insets show a typical network biased by a voltage V_+ just following the transition where the formation of a (A) conducting backbone and (B) crack may be observed.

The model we consider though, is quite general and can be applied to a variety of other materials and systems [1].

A bipolar memristor subject to an external bias will transition to a conductive state (with conductance G_{on}) in one direction and to an insulating state (with conductance G_{off}) when biased in the other. This change is generally induced by the rearrangement of ions in the applied electric field, as in the case of silver sulfide between two silver electrodes, where drifting ions form a filament structure eventually bridging the insulator [19].

These switching dynamics are typically subject to a threshold in the applied bias, below which the conductance will not vary, or will vary only slowly. When considering the dynamics of a single memristor, such thresholds may be described interchangeably in the applied voltage or current. However when embedded in a network, the two can lead to quite different dynamics. When the conductivity of an element within a network is increased, its current increases while its voltage decreases, and vice versa when its conductivity is decreased. For the electric field driven migration of vacancies or ions [20], we expect that in order to simulate the behavior of actual devices, all elements must be subject to a current rather than voltage threshold. The role of temperature has been emphasized by several studies, especially those focussing on the dissolution of the filament. Such an effect may be taken into account by the explicit inclusion of a temperature in the model, or by taking a threshold in the power dissipated in an element $P_t = GI_t^2$ which gives a current threshold that changes with the device conductance $I_t = \sqrt{\frac{P_t}{G}}$. In the discretely switching model we consider here, the two choices are identical, but when the full spectrum of memristances is allowed for, as in non-adiabatic regimes, such effects may be important.

The presence of a current threshold has immediate consequences on the dynamics of a network. As the threshold of a device in the insulating state is crossed and its

conductivity increases, more current is diverted through the element from neighboring bonds making the transition from G_{off} to G_{on} unstable. On the timescale of the slowly varying applied voltage, elements of the network will appear to switch discretely between the insulating and conducting state. Therefore, we can effectively model the elements as switching discretely from a conductance G_{off} to a conductance G_{on} , when a threshold current, $I_t > 0$, is crossed

$$G(I) = G_{off} + (G_{on} - G_{off})\theta(I - I_t), \quad (1)$$

where I is the current through the device, and $\theta(\cdot)$ is the Heaviside function of the argument.

Similar considerations would lead us to conclude that the reverse direction is ‘stable’, as passing an element’s threshold leads to a decrease in the conductance and a corresponding decrease in the current, bringing it back below the threshold. The devices would thus explore the full continuum of memristance between G_{on} and G_{off} leading to a gradual RESET-like behavior on the network level. However, we find evidence both in experimental data and simulations that this effect does not occur or is not significant in describing the behavior of the network for a wide range of parameters. For instance, in the atomic switch networks produced by Stieg *et al.* [12] sharp fluctuations in the network conductivity are observed in both directions, thought to be due to the switching of individual elements (see Fig. 3c in Ref. [12]). Such sharp behavior may be accounted for by assuming a nonlinear dependence of the conductance on the filament length due to, for example, the transition from tunneling to ballistic conductance.

Disorder at the network level can similarly render the continuum of memristive values irrelevant to the network dynamics. If the current diverted from a switching element does not cross another’s threshold, the increasing current from the boundaries will continue to transition

that element to G_{off} . As the conductance and external voltage range in which this occurs is very small relative to the network scale, this is the same as if that element had switched discretely from G_{on} to G_{off} . Simulations of networks in which the full range of memristance was accessible have not shown a significant change in dynamics and we believe the discretely switching model to be appropriate for a wide range of networks. We thus make a similar assumption for the reverse direction, obtaining the equations for an element by exchanging G_{on} with G_{off} , and I with I_t in Eq. (1) for a different threshold $I_t < 0$.

Memristive elements are also generally polar. The $Ag/Ag_2S/Ag$ atomic switches formed in atomic switch networks [5, 6] are gapless type devices (see Hasegawa *et al.* [21] for a review of types of atomic switches and their switching processes). Their symmetric metallic configuration (typically gapless switches have two differing metallic electrodes, e.g., $Ag/Ag_2S/Pt$) suggests that at the point of formation within the network, no preferred direction within the switch has been selected. Polarity is instead instilled through a ‘formation’ step in which a bias is applied to the network causing filament structures to form in the switches throughout. After a joule-heating assisted dissolution of the thinnest part of the filament, the junctions display bipolar resistive switching. The polarity of the internal switches is thus determined by the direction of current propagation from the boundaries. That this must be true in the experimental systems is evident from the fact that the network undergoes resistive switching as a whole. Without a majority of switching polarities coinciding with the direction of currents from the boundaries, the network would switch between identical states with half the switches in the G_{off} state and half in G_{on} and not display the pinched hysteresis observed in experiment. We thus assign the polarity of elements in the network to coincide with the direction of currents flowing from the boundaries.

We now turn to a network of these elements. We consider an architecture as depicted in the insets of Fig. 1, where the upper and lower boundaries of the network are held to some constant voltage or total current. The diamond lattice is chosen such that all elements participate equally in conduction and networks are periodic in the direction transverse to the current flow to mitigate finite size effects.

Including disorder is most directly done through random pruning of the lattice, however the networks produced are subject to strong finite size effects, requiring the simulation of many instances of large networks to obtain regular results. The random pruning of the lattice imposes a current distribution over the elements that is simply scaled by the external boundary conditions. This distribution determines the order in which elements cross their thresholds and is thus equivalent, at a mean-field level, to assuming a distribution in the thresholds of a

fully occupied network. It is also noted in [22] that this is obtained upon coarse-graining a randomly pruned lattice, and thus may be a better approximation to the thermodynamic limit than simulations on structurally disordered lattices. The use of a disorder distribution also affords us more direct control over the relationship between the disorder and the dynamics, simplifying the search over a large parameter space of possible structural disorders.

It is worth noting that this type of model has been arrived at in several contexts involving the interplay between conduction and disorder in 2D systems. For instance, a similar model was first applied to the study of the random fuse model for electrical failure ($G_{on} \rightarrow G_{off} = 0$) [22]. A uniform distribution of thresholds on the interval $[1 - w, 1 + w]$ was considered and behavior examined as a function of network size L and w . Brittle and ductile regimes of behavior were identified, both of which culminated in the formation of a lateral ‘crack’ severing the network. In the brittle, or narrow disorder regime, this occurred as an avalanche upon the first bond failing, while for larger w there was a regime of diffuse failure, causing the networks to progressively deform before the formation of a crack. In the thermodynamic limit, only the brittle regime survived, except for the case $w \rightarrow 1$ when the disorder distribution extended to 0. More recently, in metal-insulator transitions (MIT) [23] the $G_{off} \rightarrow G_{on}$ transition was examined for its G_{on}/G_{off} dependence, finding that a transition occurs in which the network conductivity exhibits a discontinuous jump, corresponding to the formation of a ‘bolt’. Similarly, a conducting backbone has been found to form along the direction of current flow in the case of MIT and dielectric breakdown [23] for sufficiently large values of the G_{on}/G_{off} ratio.

Interest in the dynamics of individual resistive switching (RS) devices has also led to new models such as the Random Circuit Breaker (RCB) model [24] for unipolar devices, capable of reproducing the conductivity dynamics of a unipolar device in the SET and RESET operations. In the RCB model, elements of a lattice transition to a conductive state when a voltage threshold is crossed, and back to an insulating state when another threshold is crossed in the same direction.

In view of these previous results, we thus expect the transitions observed in MIT and electrical failure studies to occur in memristive networks in the adiabatic limit. The $G_{off} \rightarrow G_{on}$ transition will correspond to the formation of a conductive backbone or ‘bolt’ through the network along the direction of current flow and the $G_{on} \rightarrow G_{off}$ transition will correspond to the formation of a ‘crack’ transverse to the direction of current flow severing the network. In both directions we anticipate a trivial brittle, or narrow disorder regime in which the transition occurs upon the first element switching and all elements transition within a narrow range of the applied

voltage, as would be the case if all elements had the same threshold. For broad disorder we expect a ductile regime in which there will be diffuse switching leading up to the transition and activity over a broad range of applied voltages. While the ductile regime does not survive in the thermodynamic limit for electrical failure, the modest size of memristive networks experimentally realized [1] suggests the ductile regime is still significant in their dynamics. Of particular interest to us is the influence of such transitions on the I-V curves of the network. From the perspective of the experimenter such effects may be desirable, such as providing strong sensitivity across a small voltage range or signaling the solution of a computational problem, or undesirable, by reducing the number of internal states accessible to the network.

Investigations of the behavior of memristive networks have been limited to date. In [13], the full time integration of a memristive network was undertaken for networks of moderate size. Elements did not include a threshold in their dynamics and the networks were investigated for their dependence on the fraction of memristive to ohmic conductors p , and their AC response. It was found that for poor ohmic conductors ($G = G_{off}$) the networks exhibited pinched hysteresis curves only when $p > 0.5$, the percolation threshold. For good ohmic conductors ($G = G_{on}$), a strongly memristive phase was observed for $p > p_c$ in which the networks switched abruptly and for $p < p_c$ a weakly memristive phase was observed, similar to that for poor ohmic conductors and $p > p_c$.

Modeling performed by [14] of the “atomic switch networks” simulated small networks including volatility and noise in their memristor model, and showed an opening of the I-V curves as the noise term was reduced and $1/f^\gamma$ ($0 \leq \gamma \leq 2$) scaling of the power spectral density for the small networks simulated ($L \approx 10$). While such studies reproduce phenomena seen in experiment, little work has been done to analyze the behavior of these models and understand how memristors in networks interact. Here, we instead focus on building an understanding of memristive networks in the adiabatic regime, where analogies with thermodynamic systems are strongest. By moderating the strength of interactions through the G_{on}/G_{off} ratio, we examine the transition that occurs in each direction and its effects on the I-V curves of the network. The features of this transition and the resulting hysteresis curves are well captured by a cluster approximation that well approximates the behavior of the network about the point of transition.

SIMULATIONS

Simulations were carried out for a square lattice at a variety of sizes, G_{on}/G_{off} ratios, and threshold distributions $p(t)$. The network dimensions were chosen such that the conductivity of the network varied from G_{off} to

G_{on} . Each element was assigned a current threshold I_t from Uniform(0, 1) in each direction, beyond which they transition from $G_{off} \rightarrow G_{on}$, or vice versa. Network dimensions were chosen so that the total network conductance varied between G_{off} and G_{on} ($N_x = N_y = 128$). The initial voltage is set to the value required to cross the lowest threshold in the network. Once that element has switched, voltages and currents are recalculated throughout the network with the external voltage held fixed, and all other elements whose currents exceed their thresholds are switched. This is repeated until no currents exceed the thresholds of their elements, at which point the voltage is raised until another threshold is crossed and this process repeated. The forward and reverse protocols are identical aside from the initial state and switching direction of the elements.

In Fig. 1 we show the network conductances as a function of applied voltage for various values of G_{on} (setting $G_{off} = 1$), in both forward $G_{off} \rightarrow G_{on}$ and backward $G_{on} \rightarrow G_{off}$ transitions, and for threshold distribution $p(t) = \text{Uniform}(0, 1)$. The displayed networks have a linear size of $N_{x/y} = 128$ memristors which we found large enough to achieve regular results over multiple realizations of the disorder. Network conductances have been scaled to lie on the interval $[0, 1]$. We note that for small values of G_{on} in both directions, the conductance is a smooth function of the voltage. As G_{on} is increased, a discontinuity forms in the slope which sharpens, appearing almost continuous until a discontinuous jump appears for large G_{on} analogous to a *first-order phase transition*. Similar behavior was seen for a variety of other distributions of sufficient breadth (not shown) with the point of transition, however, being distribution dependent. In the insulating transition, we have scaled the voltage by G_{on} such that the current densities of all networks are initially equal, bringing the transitions to the same scale in both polarities. While the dependence on G_{on}/G_{off} in the forward direction has been shown in MIT [23], we are not aware of a similar demonstration in the reverse direction, possibly as most work has focused on electrical breakdown in fuse networks in which $G_{off} = 0$.

The insets in Fig. 1 each show the configuration of a network just following a transition. In the forward transition (A), this corresponds to the emergence of a conducting backbone spanning the network. Similarly, in the reverse transition (B) a crack forms separating the network transverse to the direction of current flow.

The corresponding I-V curves are shown in Fig. 2. While the voltage scale depends only on the geometry of the network, the current scale depends on G_{on}/G_{off} and has been rescaled so that the axes coincide. The strong asymmetry of the curves is due to the use of the same threshold distribution for $G_{on} \rightarrow G_{off}$ and $G_{off} \rightarrow G_{on}$ processes. In the G_{on} state, an equivalent current will be reached for a voltage which is a factor $1/G_{on}$ lower. As there is not an obvious physical choice for how to

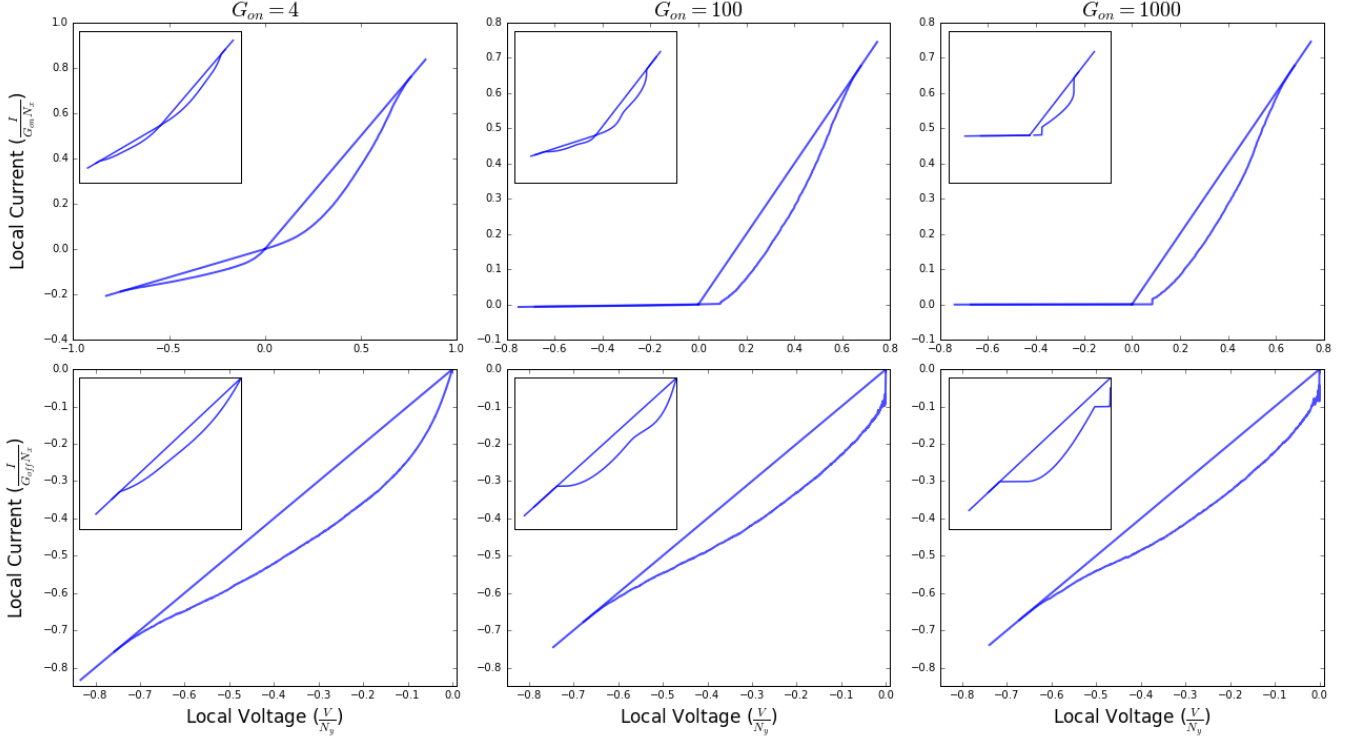


FIG. 2. Simulated hysteresis curves of memristive networks for $G_{on} = 4, 100$, and 1000 . The discrete jump in conductance becomes evident in the I-V curves for large values of G_{on} . The asymmetry of the curves is the result of element thresholds being in terms of the current, and thus the transition occurring at a factor of $1/G_{on}$ lower voltage than the corresponding forward transition. The insets show analytically reached I-V curves which demonstrate similar asymmetry and the emergence of a jump in the current. The reverse branch has been rescaled and plotted in the second row. For large G_{on} , the transition appears as a noisy area near to the y-axis. Here the jumps in conductivity at a fixed voltage give rise to sharp decreases in the current that are opposed by the subsequent increase in voltage.

connect the distributions for forward and reverse switching, we have displayed the negative voltage sections of the curves separately, on their own current scales. The discrete jump in the conductance becomes evident for sufficiently large values of G_{on} , but is less apparent than in the conductivity plots due to the long tail following the transition. Past the transition, voltage steps between thresholds become longer as current is diverted into the conducting backbone. The transition thus has an inhibitory effect on the remaining bonds, opening the hysteresis curves and spreading the memristive states over a wider voltage range. Thus, while the transition reduces the number of accessible states, it increases the resolution between those remaining.

In the second row of Fig. 2, the scaled reverse branches of the I-V curves appears remarkably similar to the positive branch, but with the roles of the current and voltage exchanged. This suggests the following mapping of the reverse branch to the forward branch,

$$V \rightarrow \frac{IN_y}{N_x G_{on}}, \quad I \rightarrow \frac{VG_{off}N_x}{N_y}, \quad (2)$$

where N_x and N_y are the lattice dimensions. In the re-

gion about the transition however, the jump of the forward branch appears as a fluctuating region in the reverse branch. Here, avalanches of transitioning elements sharply reduce the current, which is then opposed by a subsequent increase of the externally applied voltage. If we instead run the reverse branch with current-controlled boundary conditions, this fluctuating region becomes a discrete jump as seen in the first row of Figure 3. In the second row, upon the mapping (2), the curves align nearly exactly. This correspondence between the two processes is just the familiar I-V *duality* of electrical circuit theory [25]: the diamond lattice is dual to itself and taking $G \rightarrow \frac{1}{G}$ in all links takes a voltage-controlled insulator-to-metal transition to a current-controlled electrical failure process.

In the context of memristor networks, this indicates that the voltage-controlled I-V curves are dual to the current-controlled I-V curves upon exchanging the roles of voltage and current *and* the direction of the switching process. Running the model in the current controlled setting thus gives nearly identical results, but exchanges the fluctuating region in the reverse direction for the discrete jump in the forward direction.

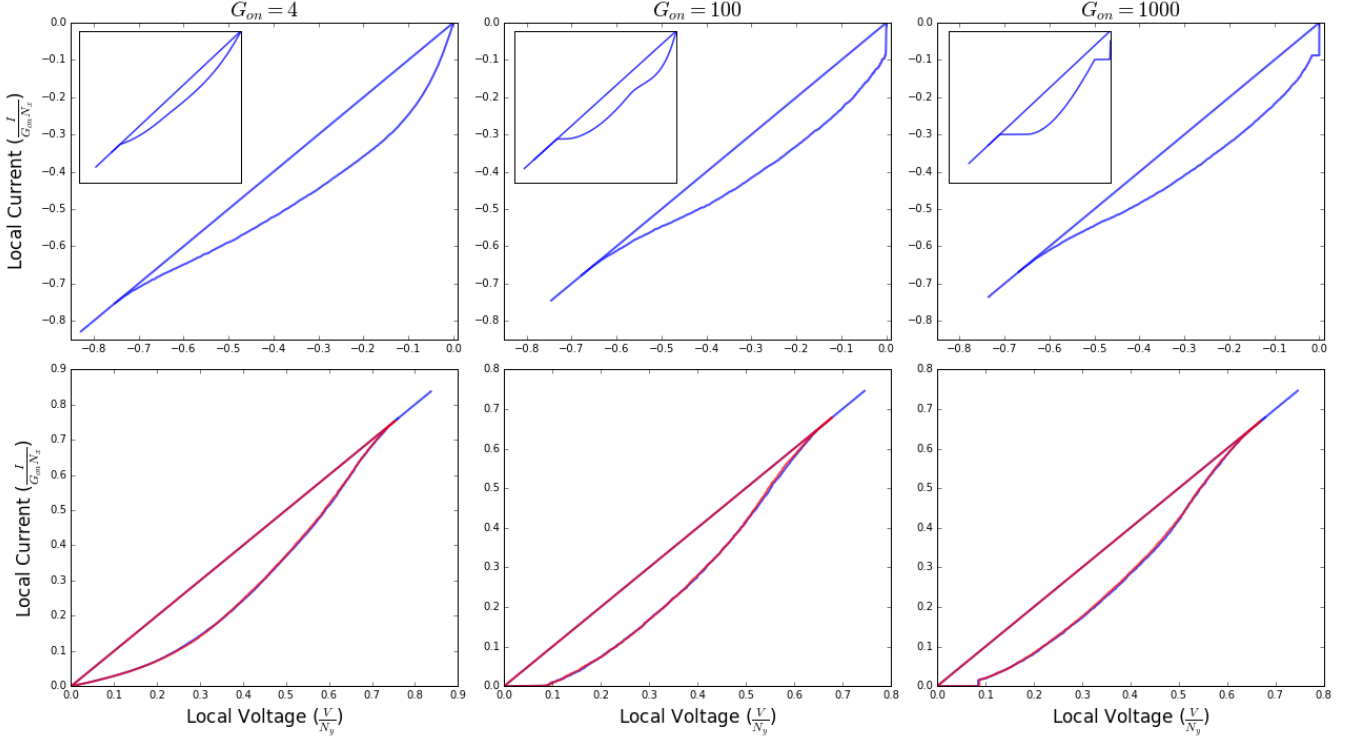


FIG. 3. For a current-controlled network switching from $G_{on} \rightarrow G_{off}$ the transition gives a discrete jump, as in the voltage-controlled $G_{off} \rightarrow G_{on}$ case. After the mapping in Eqn. 2, the reverse branch of the hysteresis curves (red) have been plotted over the forward branch for several values of G_{on} demonstrating the duality between the two processes.

It is important to note that this connection between the forward and reversed hysteresis loops has been observed experimentally in individual memristive systems [16, 17] as well. While observing the duality for a network of resistors is clear, the extension to the dynamic non-linear elements considered here is surprising, especially when considering the asymmetry in the switching process between the forward and reversed directions, one of which corresponds to a backbone forming along the direction of current propagation, and the other corresponding to a crack forming transverse to the current flow.

In the remainder of the paper, we analytically investigate our model with the aim of understanding the major features of the simulated I-V curves, namely the existence of a transition for sufficiently large G_{on}/G_{off} , the long tail following the transition, and the duality between the forward and reverse switching processes, leading to the I-V curves displayed in the insets of Figs. 2 and 3.

MEAN-FIELD THEORY

As a first step towards an analysis of the model, we develop its mean-field theory. The method followed is similar to that of Zapperi *et al.* [26] employed to analyze random fuse networks. In this form, the central phys-

ical quantity considered is the power dissipated by the network,

$$P = \sum_j g_j v_j^2 = \sum_j \frac{i_j^2}{g_j} \quad (3)$$

where g_j is the conductance of an element in the network and $v_j(i_j)$ is its voltage drop (current). We require that the average power dissipated match the power dissipated by the network $G_{net}V^2 = \frac{I^2}{G_{net}}$ and assume that all elements experience a mean-field voltage V_{MF} or current I_{MF} leading to the equations,

$$\left. \begin{array}{l} G_{net}V^2 \\ I^2 \\ G_{net} \end{array} \right\} = \left\{ \begin{array}{l} N\langle g \rangle V_{MF}^2 \\ N\langle \frac{1}{g} \rangle I_{MF}^2 \end{array} \right. \quad (4)$$

The choice of the LHS is determined by the boundary conditions applied to the network but the choice of the RHS is not constrained. An interesting form is the ‘voltage-voltage’ choice, leading to the mean-field voltage

$$V_{MF} = \sqrt{\frac{G_{net}}{\langle g \rangle}} \frac{V}{\sqrt{N}} \quad (5)$$

which unlike other choices displays a transition in both directions. To make progress we require the network conductance G_{net} . Below the transition, where switching of

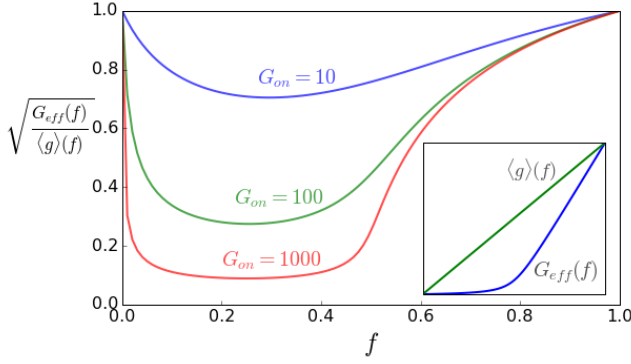


FIG. 4. $h(f) = \sqrt{\frac{G_{eff}(f)}{\langle g \rangle(f)}}$ is plotted for several values of G_{on} . In the inset, $\langle g \rangle(f)$ and $G(f)$ are plotted for $G_{on} = 100$. Note that when the average conductance increases more quickly than the network conductance as for small f , $h(f)$ is decreasing and vice versa for large f .

elements is primarily driven by the threshold distribution and not by the influence of nearby switched elements, the conductivity of the network may be well approximated by an effective medium theory, giving $G_{net} \approx G_{eff}(f)$ as a function only of the fraction of the devices in the ON state.

The functions $\langle g \rangle(f)$, $G_{eff}(f)$, and $h(f) = \sqrt{\frac{G_{eff}(f)}{\langle g \rangle(f)}}$ are plotted in Figure 4. We can understand the non-monotonic form of $h(f)$ as arising from competition between switching elements concentrating current away from other elements, and the increasing conductance of the network pulling more current in at the boundaries. For small f , the average conductance of an element is increasing faster than the network conductivity, indicating that current is concentrated away from other elements more quickly than it increases at the boundaries, and the mean-field voltage decreases. For larger f , the network conductance begins to increase more quickly than the average conductance, pulling in current faster than switching elements can concentrate it, and the mean-field voltage increases. The increasing regime at large f allows for a phase transition to occur from $G_{off} \rightarrow G_{on}$, and the decreasing portion at low f allows for the possibility of the reverse transition when the voltage is reversed.

To determine whether a transition occurs for a particular disorder distribution, we derive a self-consistency equation, ensemble-averaging over the number of elements that have switched for a given mean-field voltage. For the transition from G_{off} to G_{on} , the fraction that has switched will approach the average fraction of elements with thresholds below the mean-field voltage,

$$f = \int_0^{h(f)v} p(t) dt. \quad (6)$$

Because the applied field enters multiplicatively, the dynamics given by the mean-field theory depend only on

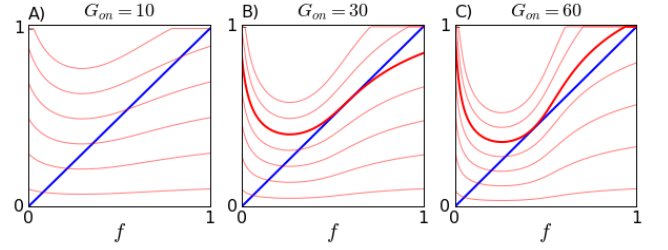


FIG. 5. The lhs (blue) and rhs (red) of Eq. (6) are plotted for several values of the applied voltage. For low values of G_{on} their intersection gives a solution that is smooth function of the voltage (panel A). A transition develops for intermediate values that can appear continuous (panel B). For sufficiently large values of G_{on} , a transition occurs where the solution jumps discontinuously. The transition voltage is highlighted in panels B) and C).

the conductance ratio G_{on}/G_{off} and is independent of the length scale of the disorder, both amounting only to a rescaling of the applied local field v . The lhs and rhs of Eq. (6) are plotted for several values of the voltage in Figure 5. For the chosen distribution and G_{on}/G_{off} ratios a transition is evident at the point

$$1 = p(h(f)v)h'(f)v \quad 0 \leq f \leq 1. \quad (7)$$

We also note that the inflection of the curves from the RHS of Eq. (6) shows a trend that looks almost like a continuous transition, corresponding to the behavior seen in simulations for intermediate values of G_{on} (see Figure 1).

An exactly analogous treatment may be undertaken for the transition from $G_{on} \rightarrow G_{off}$. We regard $f_R = 1 - f$ as the fraction of devices in their G_{off} state and $v = \frac{V}{\sqrt{N}}$ as the positive voltage applied in the *reverse* direction. The effective medium conductivity may be obtained from the substitution $f \rightarrow 1 - f_R$, $G_{eff,R}(f_R) = G_{eff}(1 - f_R)$ and similarly with the average conductivity $\langle g \rangle_R(f_R) = \langle g \rangle(1 - f_R)$, giving a mean field voltage $V_{MF} = h_R(f_R)v = \sqrt{\frac{G_{eff,R}(f_R)}{\langle g \rangle_R(f_R)}}v$. As the mechanisms for turning ON and OFF within the individual atomic switches are not the same, we take a possibly different probability distribution $p_R(t)$ for the reverse switching thresholds. With these definitions we obtain the self-consistency equation as before,

$$f_R = \int_0^{h_R(f_R)v} p_R(t) dt. \quad (8)$$

In Fig. 5 this quantity has been plotted for several values of G_{on} and the applied voltage. We observe a first-order phase transition similar to that observed in the $G_{off} \rightarrow G_{on}$ branch. However, this transition occurs for much lower values of G_{on} and near the limiting value of

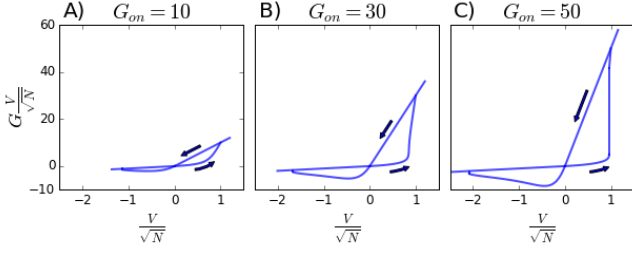


FIG. 6. Solving the self consistency equations (6) and (8) for a uniform distribution leads to the hysteresis curves above. For small values of G_{on}/G_{off} , the networks are smooth, but as the ratio is increased a discrete jump emerges in the forward direction. A similar jump near the end of the reverse branch is only barely discernible.

the conductance. As we proceed from $f = 1$ to 0, in the vicinity of $f = 0$ the average conductance $\langle g \rangle(f)$ is decreasing more rapidly than the network conductance $G_{eff}(f)$. This leads the internal switches to redistribute current to their neighbors faster than the decrease of the total current at the boundary. This increases the mean-field voltage overall, and hence promotes a transition.

Solving the self-consistency equations gives the mean-field hysteresis curves plotted in Fig. 6. While these curves display a qualitative similarity to simulation, several features of the mean-field theory are lacking. As we have already noted, the choice for the form of the mean-field theory (voltage-voltage, current-voltage, etc.) are not prescribed *a priori* and each choice will give a slightly different account of the dynamics. All of these share the feature that transitions occur due to competition between a changing current at the boundaries and the internal sharing of currents within the network, as summarized by the function $h(f)$ which is some ratio between the network conductance and an average conductance $\langle g \rangle$, $\langle \frac{1}{g} \rangle$. In both directions, the transition will eventually proceed (as $G_{on} \rightarrow \infty$) from some critical fraction f_c to a fully switched network $f = 1$ as opposed to the finite jump and long tail seen in simulations.

Having observed the internal form of the transition in simulation, we can see that in contrast to thermal transitions, where the phase transition occurs homogeneously throughout the system, the conductivity transitions consist only of a $d = 1$ dimensional conducting backbone in the forward direction and a $d = D - 1$ dimensional crack in the reverse. In $D = 2$ both of these correspond to one dimensional subsystems of the network and so the mean-field theory which considers all elements equally cannot model it accurately, especially in the regime following the formation of the backbone. In the following, we consider methods for modeling the formation of the backbone.

1D MODELS

The mean-field assumption, that all elements experience either a voltage V_{MF} or current I_{MF} , is equivalent to replacing the network with a 1D parallel or series arrangement of memristors whose boundary conditions are then matched (through an effective medium theory) to the behavior of the original network. In fact, the quantities

$$\langle g \rangle = G_{off} + \frac{n}{N}(G_{on} - G_{off}) \quad (9)$$

$$\left\langle \frac{1}{g} \right\rangle = \frac{G_{on} + \frac{n}{N}(G_{off} - G_{on})}{G_{on}G_{off}} \quad (10)$$

which appear in the mean-field equations (4) are also the conductances G_{net}/N for a series and parallel network of N memristors with n in the ON state. Having seen that the transition is restricted to a small subset of the network, we do not expect that including the entire network in the backbone will capture the behavior in the vicinity of the transition (where homogeneity, and thus the effective medium theory, fails). We thus first explore the opposite extreme by ignoring the presence of the rest of the network and considering only those elements involved in the conducting backbone or crack.

In the forward direction, the transitioning elements are a collection of memristors in series of length N_y held at a voltage V . Such an arrangement with a fraction f in the ON state admits a current,

$$I(f) = \frac{G_{on}G_{off}}{G_{on} + f(G_{off} - G_{on})} \frac{V}{N} \quad (11)$$

and the fraction of elements in the ON state may be determined self-consistently,

$$f = \int_0^{I(f)} \rho(t) dt. \quad (12)$$

The distribution $\rho(t)$ is the distribution of thresholds in the conducting backbone which should be related to the distribution of thresholds across the network. While an explicit calculation of ρ is difficult, a reasonable approximation on the diamond lattice should be $\rho(t) = 2p(t)(1 - F(t))$ where $F(t)$ is the cumulative distribution function of the threshold distribution, such that the current always selects the path with lower threshold. We note that this concentrates the threshold distribution towards its lowest values but does not strongly alter the behavior of the theory. In the interest of simplicity, we thus maintain our use of the Uniform(0, 1) distribution in illustrating the features of each approach. Equation (12) is plotted in Fig. 7 for several values of G_{on} in which we observe the transition first occurring at $G_{on} = 2$, and then progressing to a jump to $f = 1$ for larger values.

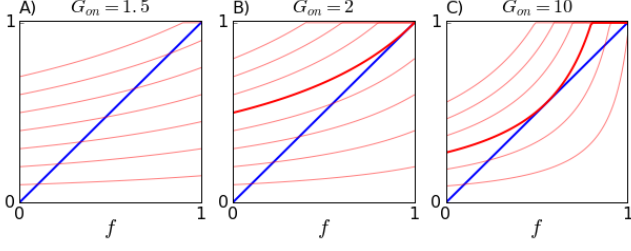


FIG. 7. The lhs (blue) and rhs (red) of Eq. (12) are plotted for several values of the applied voltage for the distribution Uniform(0,1). For a collection of memristors in series, the transition is the completion of the conducting backbone, with all elements in the G_{on} state.

In the reverse direction, we consider a collection of memristors in parallel of length N_x corresponding to the crack that will eventually sever the network. As the ‘crack’ is separated from the boundaries, the boundary conditions are instead supplied by the network. As every strip of memristors perpendicular to the direction of current propagation will have a current $G_{net}V$ passing through them, the reverse switching process of a voltage-controlled network should be best described by a current-controlled strip of memristors in parallel. For the moment, we again ignore the presence of the rest of the network and consider an isolated set of elements. The conductance of the 1D strip of memristors in parallel with a fraction f_R in the G_{off} state is

$$N(G_{on} + f_R(G_{off} - G_{on})) \quad (13)$$

which gives the current through an element in the ON state,

$$I(f_R) = \frac{G_{on}G_{net}}{G_{on} + f_R(G_{off} - G_{on})} \frac{V}{N}. \quad (14)$$

f_R may be similarly found self-consistently

$$f_R = \int_0^{I(f_R)} \rho(t) dt. \quad (15)$$

The resulting mean-field theory is just the reverse of that for the forward switching process (taking $G_{net} = G_{on}$) but with a voltage scale smaller by a factor of G_{on} .

Here, physical considerations from the switching processes have led us to two *dual* structures: a series chain of memristors transitioning from $G_{off} \rightarrow G_{on}$ subject to a ramped voltage as a model of the conducting backbone, and a parallel strip of memristors transitioning from $G_{on} \rightarrow G_{off}$ subject to a ramped current for the crack severing the network. Each of these demonstrates a transition in which the networks proceed from some $f = f_c$ to $f = 1$ at a critical voltage or current.

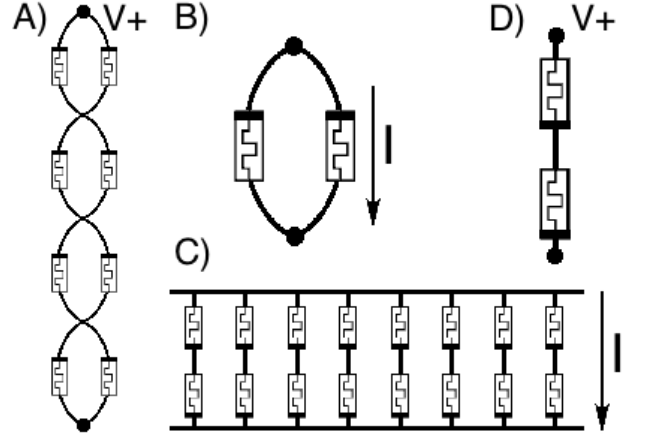


FIG. 8. The systems and sub-units considered in the cluster approximations. As a model of the conducting backbone embedded in the network we consider (A) a series ‘chain’ of memristors in parallel subject to a slowly ramped voltage $V+$ composed of sub-units of (B) pairs of memristors in parallel subject to a slowly ramped current. As a model of the crack, we consider (C) a parallel strip of memristors in series subject to a slowly ramped current consisting of sub-units of (D) pairs of memristors in series subject to a slowly ramped voltage.

CLUSTER MODELS

In order to include the influence of the conducting backbone or crack on the rest of the network and thus the behavior of the network past the transition, we use a cluster approach similar to the Bethe-Kikuchi approximation in equilibrium thermodynamics [27, 28]. To this end we replace each memristor in the series chain with two memristors in parallel as in Figure 8 A and subject the entire chain to a slowly ramped voltage. Each pair in the chain is thus subject to a current I slowly raised from zero (See Fig. 8 B). If the threshold of each memristor, t_i is drawn independently from a distribution $p(t)$, the probability distribution for the conductance of the pair $G_{||}$ is,

$$\begin{aligned} p(2G_{off}; I) &= 2 \int_{I/2}^{\infty} dt_1 \int_{t_1}^{\infty} dt_2 p(t_1)p(t_2) \\ p(G_{off} + G_{on}; I) &= 2 \int_{\frac{G_{off}I}{G_{off}+G_{on}}}^{I/2} dt_1 \int_{t_1}^{\infty} dt_2 p(t_1)p(t_2) \\ &\quad + 2 \int_0^{\frac{G_{off}I}{G_{off}+G_{on}}} dt_1 \int_{\frac{G_{off}I}{G_{off}+G_{on}}}^{\infty} dt_2 p(t_1)p(t_2) \\ p(2G_{on}; I) &= 2 \int_0^{\frac{G_{off}I}{G_{off}+G_{on}}} dt_2 \int_0^{t_2} dt_1 p(t_1)p(t_2). \end{aligned} \quad (16)$$

A long chain of such pairs in series (Fig. 8 A), each with conductance $G_{||,i}$ will possess a total conductance close

to

$$\left\langle \frac{1}{G_{chain}} \right\rangle = N \left\langle \frac{1}{G_{\parallel}} \right\rangle \quad (17)$$

and we may determine the current through the chain self-consistently as the smallest solution of the equation

$$\frac{V/N_x}{I} = \left\langle \frac{1}{G_{\parallel}} \right\rangle \quad (18)$$

where the I dependence of $\langle \frac{1}{G_{\parallel}} \rangle$ has entered through the averaging. Using again the distribution $\text{Uniform}(0,1)$, the solution to this equation has been plotted in the insets of Figs. 2 and 3 for several values of G_{on} .

Here, we see the finite jump in conductance observed in simulations followed by the gradual switching of the remaining memristors. This is due to the memristor in the ON state diverting current away from its neighbor. While a current of only $I = 2$ (in units of $G_{off}V$) is required to switch the first of the pair, a current of $I \approx (G_{on} + G_{off})/G_{off}$ is required to guarantee the switching of the second, which for large values of G_{on}/G_{off} is considerable.

An analogous treatment of the reversed switching process requires replacing each element of the parallel strip of memristors with two elements in series (Fig. 8 C) subject to a slowly ramped current. Each pair is then subject to a slowly ramped voltage V (Fig. 8 D). Again drawing the thresholds independently from a distribution $p(t)$, the distribution for the conductance of the pair is

$$\begin{aligned} p\left(\frac{G_{on}}{2}; V\right) &= 2 \int_{G_{on}V/2}^{\infty} dt_1 \int_{t_1}^{\infty} dt_2 p(t_1)p(t_2) \\ p\left(\frac{G_{on}G_{off}}{G_{on} + G_{off}}; V\right) &= 2 \int_{\frac{G_{on}G_{off}V}{G_{off} + G_{on}}}^{G_{on}V/2} dt_1 \int_{t_1}^{\infty} dt_2 p(t_1)p(t_2) \\ &\quad + 2 \int_0^{\frac{G_{on}G_{off}V}{G_{off} + G_{on}}} dt_1 \int_{\frac{G_{on}G_{off}V}{G_{off} + G_{on}}}^{\infty} dt_2 p(t_1)p(t_2) \\ p\left(\frac{G_{off}}{2}; V\right) &= 2 \int_0^{\frac{G_{on}G_{off}V}{G_{off} + G_{on}}} dt_2 \int_0^{t_2} dt_1 p(t_1)p(t_2). \end{aligned} \quad (19)$$

A strip of N_y of these, each with conductance $G_{series,i}$, in parallel (Fig. 8 C) will have conductance $N_y \langle G_{series} \rangle$. As discussed above, such a strip embedded within a network will be subject to a current I and thus satisfy

$$N_y \langle G_{series} \rangle V = I, \quad (20)$$

where the voltage across the strip is determined self-consistently as the smallest solution of the above equation and the voltage dependence of $\langle G_{series} \rangle$ has entered through the averaging over the voltage dependent distribution above.

The two structures considered above are again *dual* and while the self-consistency equation may be solved as before, we instead note that the exchange

$$V \rightarrow \frac{IN_y}{N_x G_{on}}, \quad I \rightarrow \frac{VG_{off}N_x}{N_y} \quad (21)$$

takes the above self-consistency equation, to that of the forward switching process (we consider a square network $N_x = N_y = N$ to avoid dimensional factors)

$$N \langle G_{series} \rangle V = I \rightarrow \frac{V/N}{I} = \left\langle \frac{1}{G_{\parallel}} \right\rangle \quad (22)$$

The reversed switching process thus maps exactly to the forward switching process upon exchanging the roles of the voltage and current and scaling appropriately, as seen in the simulated I-V curves of Figure 3.

MEAN-FIELD DYNAMICS

Although the avalanche dynamics of mean-field models akin to the random-field Ising model are well known [29], we include here a brief discussion in the interest of completeness.

The mean-field theories considered lead to self-consistency equations of the form

$$f = \int_0^{h(f)v} p(t) dt \quad (23)$$

where v is an external field and $h(f)$ is some function of the fraction of switched elements f . We consider this relation to be initially satisfied and raise the voltage until the next threshold is passed. This takes $f \rightarrow f + \frac{1}{N}$, increasing the limit of (23) by $\frac{h'(f)v}{N}$. The probability that n memristors are switched ON by this increase is given by a Poisson distribution

$$p_n = \frac{\mu^n}{n!} e^{-\mu}, \quad \mu = p(h(f)v)h'(f)v. \quad (24)$$

Each of the n memristors will cause a similar increase in the mean-field voltage, and thus will give rise to the same distribution. Therefore, by switching a single memristor gives rise to a poissonian branching process. This may be brought into a more useful form by calculating the total number of memristors switched in a single branching process, or the avalanche size distribution. This leads to the Borel distribution

$$p_S = \frac{(\mu S)^{S-1}}{S!} e^{-\mu S}, \quad S = 1, 2, \dots \quad (25)$$

with $\mu = p(h(f)v)h'(f)v$. This distribution has mean and variance,

$$\langle S \rangle = \frac{1}{1 - \mu}, \quad \sigma_S^2 = \frac{\mu}{(1 - \mu)^3}. \quad (26)$$

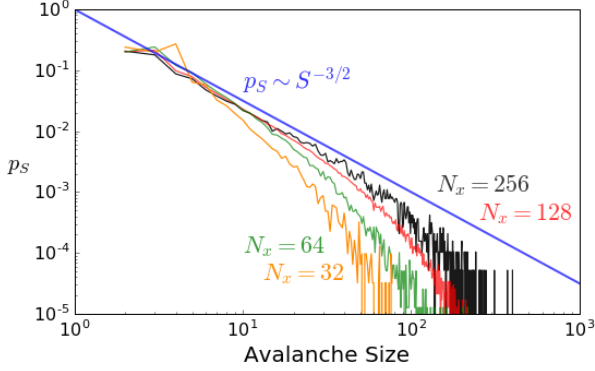


FIG. 9. Avalanche sizes binned just above the transition for randomly diluted networks ($p = 0.6$, $G_{on} = 100$) of size $N_{x/y} = 32, 64, 128$ (1000 realizations) and $N_{x/y} = 256$ (100 realizations). As the network size increases, the avalanche size distribution approaches the asymptotic form $P(s) \sim s^{-3/2}$ given by the mean-field theory, subject to a finite size cut-off.

and therefore the mean-field dynamics give avalanches whose size is determined by the parameter μ .

For $\mu < 0$, raising the voltage will cause individual memristors to switch and no avalanches will occur, corresponding to a diffuse regime. For $0 < \mu < 1$, the system will display avalanches of finite size according to the Borel distribution. At $\mu = 1$, the system reaches a critical branching process, at which point the probability of an infinite avalanche begins to grow and the distribution approaches the limiting form $p_s \sim s^{-3/2}$.

The conductance jumps that the system experiences for avalanches in the regime $0 < \mu < 1$ should be approximately $G'_{net}(f) \frac{S}{N}$ and thus, for a particular value of the conductance, conductance jumps in that vicinity should follow a Borel distribution. Such jump avalanche distributions have been well studied both numerically [23] and in experiment [30] for individual memristive elements but not yet disordered systems consisting of many memristive elements, such as those of Stieg *et al.* [6].

In order to confirm whether this scaling law would be accessible in experiments for physically disordered lattices, we have simulated randomly diluted lattices (by removing bonds above percolation) without threshold disorder as the effect of spatial correlations may modify the behavior. Avalanches were binned in the region surrounding the peak in the avalanche size for various sizes of the networks. The histograms produced are plotted in Figure 9. As the system size increases, the histograms approach the form predicted by the mean-field theory, although clearly subject to a finite-size cutoff.

CONCLUSIONS

We have presented a simple model that captures the behavior of a disordered two-dimensional memristive network when subject to bias in the adiabatic limit. As the memristive G_{on}/G_{off} ratio is increased, the conductivity changes from a smooth function of the applied voltage to displaying a discontinuous jump as in a *first-order phase transition*. Internally, this is due to the formation of a conducting backbone or crack through the network. While the I-V curves demonstrate such a jump, the restriction of the transition to a small subset of the network elements moderates its size to a fraction of the network conductivity. Furthermore, the current diverted from the rest of the network extends the voltage range of the remaining memristors, maintaining the voltage range of the network.

The $G_{on} \leftrightarrow G_{off}$ processes are connected by a *duality* that maps the hysteresis curves of a voltage-controlled network to those of a current-controlled network in the opposite polarity. A cluster approximation duplicates this behavior and reveals that, in order to fully transition the network, elements of the backbone will need to carry currents a factor G_{on}/G_{off} larger than their neighbors. As filament-type memristive devices have both large G_{on}/G_{off} ratios and are sensitive to the maximum current through them, this may limit the operating voltages of computational devices manufactured from memristors to the neighborhood of the transition. Fortunately, this seems to be the region in which the dynamics of the networks carry the greatest promise for the design of computational devices, as seen in maze and shortest path solvers [8] where the transition may correspond to the solution of an optimization problem. We hope this work will provide a foundation to extend the understanding of these networks to the non-adiabatic regime in which their behavior may be substantially more complex and interesting.

We thank G. Pruessner, S. Peotta, F. Caravelli, and F. Traversa for useful discussions and acknowledge partial support from the Center for Memory Recording Research at UCSD.

* fsheldon@ucsd.edu

† diventra@physics.ucsd.edu

- [1] Y. V. Pershin and M. Di Ventra, Adv. Phys. **60**, 145 (2011).
- [2] T. Hasegawa, T. Ohno, K. Terabe, T. Tsuruoka, T. Nakayama, J. K. Gimzewski, and M. Aono, Adv. Mater. **22**, 1831 (2010).
- [3] T. Ohno, T. Hasegawa, T. Tsuruoka, K. Terabe, J. K. Gimzewski, and M. Aono, Nat. Mater. **10**, 591 (2011).
- [4] D. R. Chialvo, Nat. Phys. **6**, 744 (2010).
- [5] A. V. Avizienis, H. O. Sillin, C. Martin-Olmos, H. H.

- Shieh, M. Aono, A. Z. Stieg, and J. K. Gimzewski, PLoS One **7**, e42772 (2012).
- [6] A. Stieg and A. Avizienis, Jpn. J. Appl. Phys. **02** (2014).
- [7] M. D. Ventra and Y. Pershin, Nat. Phys. **9**, 200 (2013).
- [8] Y. V. Pershin and M. Di Ventra, Phys. Rev. E **88**, 013305 (2013).
- [9] F. L. Traversa, C. Ramella, F. Bonani, and M. Di Ventra, Sci. Adv. **1**, e1500031 (2015).
- [10] F. L. Traversa and M. Di Ventra, IEEE Trans. Neural Networks Learn. Syst. **26**, 1 (2015).
- [11] C. Langton, Phys. D Nonlinear Phenom. **42**, 12 (1990).
- [12] A. Stieg and A. Avizienis, Adv. Mater. **24**, 286 (2012).
- [13] E. Nedaee Oskoei and M. Sahimi, Phys. Rev. E **83**, 031105 (2011).
- [14] H. O. Sillin, R. Aguilera, H.-H. Shieh, A. V. Avizienis, M. Aono, A. Z. Stieg, and J. K. Gimzewski, Nanotechnology **24**, 384004 (2013).
- [15] M. Di Ventra and Y. V. Pershin, Nanotechnology **24**, 255201 (2013).
- [16] I. H. Inoue, S. Yasuda, H. Akinaga, and H. Takagi, Phys. Rev. B - Condens. Matter Mater. Phys. **77**, 1 (2008).
- [17] P. K. Sarswat, Y. R. Smith, M. L. Free, and M. Misra, ECS J. Solid State Sci. Technol. **4**, Q83 (2015).
- [18] H. O. Sillin, E. J. Sandouk, A. V. Avizienis, M. Aono, A. Z. Stieg, and J. K. Gimzewski, J. Nanosci. Nanotechnol. **14**, 2792 (2014).
- [19] Z. Xu, Y. Bando, W. Wang, X. Bai, and D. Golberg, ACS Nano **4**, 2515 (2010).
- [20] M. Di Ventra, *Electrical transport in nanoscale systems*, Vol. 14 (Cambridge University Press Cambridge, 2008).
- [21] T. Hasegawa, K. Terabe, T. Tsuruoka, and M. Aono, Adv. Mater. **24**, 252 (2012).
- [22] B. Kahng, G. G. Batrouni, S. Redner, L. De Arcangelis, and H. J. Herrmann, Phys. Rev. B **37**, 7625 (1988).
- [23] A. Shekhawat, S. Papanikolaou, S. Zapperi, and J. P. Sethna, Phys. Rev. Lett. **107**, 1 (2011).
- [24] S. C. Chae, J. S. Lee, S. Kim, S. B. Lee, S. H. Chang, C. Liu, B. Kahng, H. Shin, D. W. Kim, C. U. Jung, S. Seo, M. J. Lee, and T. W. Noh, Adv. Mater. **20**, 1154 (2008).
- [25] T. Iyer, *Circuit Theory* (Tata McGraw-Hill, New Delhi, 1985) pp. 206–212.
- [26] S. Zapperi, P. Ray, H. E. Stanley, and A. Vespignani, Phys. Rev. E **59**, 5049 (1999).
- [27] H. A. Bethe, Proc. R. Soc. London A **150**, 552 (1935).
- [28] R. Kikuchi, Phys. Rev. **81**, 988 (1951).
- [29] J. P. Sethna, K. Dahmen, S. Kartha, J. A. Krumhansl, B. W. Roberts, and J. D. Shore, Phys. Rev. Lett. **70**, 3347 (1993).
- [30] A. Sharoni, J. G. Ramírez, and I. K. Schuller, Phys. Rev. Lett. **101**, 4 (2008).